Stochastic properties of a four-vortex system

E. A. Novikov and Yu. B. Sedov

Institute of Atmospheric Physics, USSR Academy of Sciences
(Submitted 31 January 1978)
Zh. Eksp. Teor. Fiz. **75**, 868–876 (September 1978)

It is established that the trajectories of a vortex system exhibits local exponential divergence if the motion is not quasiperiodic. It is shown by the same token that two-dimensional flow of an ideal fluid (or of a plasma in a magnetic field) is in general not a completely integrable system. The global stochastic properties (ergodicity and mixing) of a vortex system, which correspond to some natural division of phase space into fourteen cells, are investigated.

PACS numbers: 47.10. + g

We formulate here a number of questions of interest in the modern theory of turbulence. Is turbulent flow in the general case stochastic[1] (does it have the property of mixing in phase space)? If it is stochastic, does it remain so in the absence of viscosity, when an integral of the energy is obtained? This question is particularly vital for two-dimensional flow of an ideal liquid, when the vorticity in the liquid particles is additionally conserved. Is this two-dimensional flow of an ideal liquid a completely integrable system in the sense established for the Korteweg–de Vries equations[2]? Finally, if stochastization does take place, what is the minimum number of degrees of freedom characterizing the flow?

We note that the models obtained when the hydrodynamic equations are truncated by projection on a certain finite system of functions (e.g., Ref. 3) cannot answer the foregoing questions, since they do not correspond to the exact hydrodynamic equations. To demonstrate with a particular example that turbulent flow, generally speaking, is stochastic it is necessary to find for the exact hydrodynamic equations a solution that possesses this property.

As is frequently the case in mathematics, when searching for a general theorem it is convenient to expand the class of solutions by forgoing the smoothness requirement. In this sense, a useful model of two-dimensional turbulence is a system of linear vortices.[4] Such vortices, as is well known, play a fundamental role in superfluidity and superconductivity phenomena, and are widely used in the simulation of various non-smooth flows as well as of plasma in a magnetic field.

Thus, is a system of vortices stochastic, and if so, what is the minimum number of vortices necessary for stochastization? According to Helmholtz, two vortices rotate uniformly. The equations for a system of three vortices can be integrated by numerical quadrature. The relative motion of three identical vortices is almost always periodic (the absolute motion is quasiperiodic), with the exception of one value of a decisive dimensionless parameter, at which the motion is aperiodic and unstable. In the present paper, making use of numerical experiments, we show that a system of four vortices has stochastic properties. The results are used in Sec. 5 to draw certain conclusions in light of the questions raised above.

1. SYSTEM OF FOUR VORTICES

We consider, on an infinite plane, four point vortices with intensities (circulations of the velocity around the vortices) $\varkappa_\alpha$ ($\alpha=1,\ldots,4$).

The Cartesian coordinates $x_i^{(\alpha)}(t)$ ($i=1, 2$) of the vortices satisfy a system of Hamilton equations,[5] which we write in the form

$$\varkappa_\alpha \frac{dx_i^{(\alpha)}}{dt} = \varepsilon_{ij} \frac{\partial H}{\partial x_j^{(\alpha)}} = -\frac{\varepsilon_{ij}}{2\pi} \sum_\beta{}' \frac{\varkappa_\alpha \varkappa_\beta (x_j^{(\alpha)} - x_j^{(\beta)})}{l_{\alpha\beta}^2}, \qquad (1.1)$$

$$H = -\frac{1}{2\pi} \sum_{\alpha<\beta} \varkappa_\alpha \varkappa_\beta \ln l_{\alpha\beta} = \text{const}. \qquad (1.2)$$

Here ε_{ij} is an anti-symmetrical tensor ($\varepsilon_{12}=-\varepsilon_{21}=1$, $\varepsilon_{11}=\varepsilon_{22}=0$), with summation from 1 to 2 over the Latin indices, $l_{\alpha\beta}$ is the distance between the vortices, and the prime on the summation sign means that the term with $\alpha=\beta$ is omitted. The quantity H has the meaning of the interaction energy of vortices and is an integral of the motion. The invariance of H relative to shifts and rotation of the reference frame leads to additional three integrals of the motion:

$$Z_i = \sum_\alpha \varkappa_\alpha x_i^{(\alpha)}, \qquad (1.3)$$

$$I = \sum_\alpha \varkappa_\alpha (x_i^{(\alpha)})^2. \qquad (1.4)$$

It is useful to use also a combination of the invariants Z_i and I (Ref. 4):

$$M = \sum_{\alpha,\beta} \varkappa_\alpha \varkappa_\beta (x_i^{(\alpha)} - x_i^{(\beta)}) = 2I \sum_\alpha \varkappa_\alpha - 2Z_i^2. \qquad (1.5)$$

The integrals (1.3)–(1.5), naturally, are in involution with H (in the calculation of the Poisson brackets it is necessary to choose the quantities $|\varkappa_\alpha|^{1/2} x_i^{(\alpha)}$ as the canonical variables). The integrals (1.3) and (1.4), however, are not involution with each other. Thus, the four independent integrals (1.2)–(1.4) are insufficient to integrate the system of four vortices by standard methods of Hamiltonian mechanics.[6]

We note that in the case of vortices of like sign the quantities M, I, and Z_i^2 are in involution. Using two of these quantities in H, we can integrate the system of three vortices of like sign by the standard methods indicated above. It is more convenient, however, to integrate the system of three vortices (both of like sign and of opposite signs) after first considering the

 0038-5646/78/090440-05$02.40

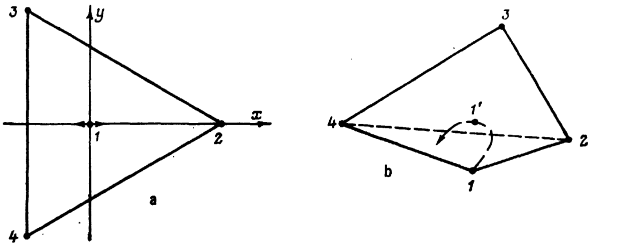

FIG. 1. Vortex configurations: a—initial configuration for numerical experiments (the arrows indicate the directions of the initial displacements), b—typical convex and nonconvex configurations and transitions between them.

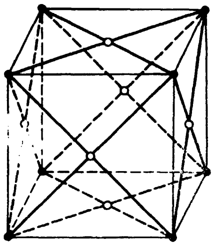

FIG. 2. Graph for transitions between different configurations.

relative motion of the vortices.[4]

There are a number of particular cases when a system of four vortices can be integrated. Foremost among them are symmetrical configurations. If a vortex of arbitrary intensity is placed in the center of an equilateral triangle with identical vortices at its vertices (Fig. 1a), then the system will rotate rigidly around the central vortex (we shall show later on that such a motion is unstable for four identical vortices, see also Ref. 7). Four identical vortices located at the vertices of a square will also rotate rigidly. The question of the motion of four vortices that have pairwise equal intensities and are symmetrically arranged about the center of gravity can be integrated in analogy with the problem of three vortices.[4]

Other integrable particular cases involve configurations with noncommensurate distances between the vortices. For example, if two vortices lie very close to each other, then they can be replaced, in first-order approximation, by one vortex whose intensity is the sum of the two, and corrections can then be introduced by perturbation theory. The case when one vortex is located far from a group of three vortices is treated similarly.

We shall be interested in the motion of four identical vortices with commensurate distances between them. The configuration of the four vortices are determined by five parameters (for example, the distances between different vortices). The integrals (1.2) and (1.5) make it possible to decrease the number of independent variables to three. We shall not write out here the obtained system of three equations for the relative motion of the vortices, since it is too cumbersome. We note only that when the type of the vortex configuration is changed, the signs of the different terms of these equations change, so that the problem must be solved "piecewise." A similar circumstance takes place also in the simpler problem of three vortices.[4] This suggests an abbreviated description of the system of four vortices with the aid of the natural phase-space subdivision, proposed below.

2. SUBDIVISION OF PHASE SPACE

The different types of configurations of a system of four vortices can be grouped into two classes–nonconvex (when one of the vertices is inside the triangle made up by the remaining vortices) and convex (Fig. 1b). The boundaries between these two classes are configurations of three vortices on a single straight line. The class of nonconvex configurations breaks up in turn into seven types. In fact, any one of the four vortices can be located inside the triangle, and the remaining three vortices can have two different orientations depending on how the vortices are numbered around the triangle, e.g., counterclockwise (compare with the three-vortex problem).[4] The class of concave configurations breaks up into six types that differ in the permutation of three vortices with one remaining fixed.

We note that when the vortices move the system cannot go over directly from one form of configuration to another of the same class. Nonconvex configurations can go over directly only into convex ones, and vice versa. Further, each nonconvex configuration can go over into only one of its three conjugate convex configurations, wherein the central vortex crosses one of the sides of the triangle (Fig. 1b). Each convex configuration can go over into one of four nonconvex configurations when one of the vortices turns out to be inside the triangle (with the orientation of the remaining three vortices unchanged).

It is convenient to represent the different transitions between the configurations in the form of a graph (diagram). This graph is planar[1)] and it is convenient to place it on the surface of a cube (Fig. 2). The vertices of the cube correspond to the nonconvex configurations, and the centers of the faces correspond to the convex configurations. In each "step" the system traverses half the diagonal of the corresponding space of the cube.

Thus, in the abbreviated description, the system can be in one of 14 states. An analysis of the behavior of the system reduces to a study of the sequence of the states and of the corresponding times.

3. NUMERICAL EXPERIMENTS

As the initial conditions for the numerical experiments we chose the configuration shown in Fig. 1a. In the unperturbed states, the system rotates about the central vortex with a period $T = 2\pi^2 R^2/\varkappa$, where R is the distance from the central vortex to the vertices of the regular triangle of the remaining vortices. The origin of the coordinates was placed at the center of the regular triangle, and the abscissa axis is drawn through one of the vertices. The unit length is chosen to be the distance R.

It is known (see, e.g., Ref. 8), that one of the causes

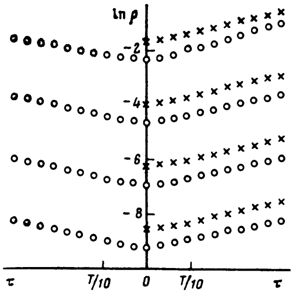

FIG. 3. Exponential acceleration of trajectories in a system of vortices.

of the stochasticity is local instability of the motion. To investigate the instability we traced the time dependence of the distances between the different trajectories in an eight-dimensional phase space (the coordinates of the four vortices) with Euclidean metric. The initial conditions were specified by shifting the central vortex along the abscissa axis by an amount $\varepsilon = \pm\varepsilon_m$ ($\varepsilon_m = R\cdot 10^{-m}$, $m=4,3,2,1$).

The system of ordinary differential equations (1.1) was integrated with a computer by the Runge–Kutta method to fourth order of accuracy. The integration was with constant time intervals equal to $T/160$ (it was assumed here that $\varkappa = 2\pi$, corresponding to $T=\pi$). The integrals of motion (1.2)–(1.4) were used to check the accuracy.

The results shown in Fig. 3 indicate that in our case local exponential instability sets in. The circles of Fig. 3 mark the logarithms of the distances between the unperturbed trajector ($\varepsilon=0$) and the trajectories with perturbations $\varepsilon=\varepsilon_m$ (in the right-hand half of the plot) and $\varepsilon=-\varepsilon_m$ (in the left half), and the crosses correspond to the distances between the trajectories with $\varepsilon=\varepsilon_m$ and $\varepsilon=-\varepsilon_m$ ($m=4,3,2,1$). The instability growth rate turned out to be of the order of unity (in the time-scale $2\pi R^2/\varkappa$ chosen as indicated above).

To study the global properties of the system of four vortices over a long time, we observed the behavior of the trajectories with initial perturbations $\varepsilon=\pm\varepsilon_1$. We noted in which of the cells of the phase space (Sec. 2) the trajectory was located, and how long it stayed there. This procedure corresponds in fact to the method of "symbolic dynamics" (see, e.g., Ref. 9).

The experiment was broken up into stages, each containing 700 realizations of successive states (cell numbers). For each stage we calculated the relative frequency (probability) of a trajectory landing in each cell, and the total time spent in it, as well as the probability matrices of the k-step transitions. Observation of the trajectories was carried out over 24 stages (almost 1.7×10^4 transitions between cells) in a time $\sim 1.4\times 10^4\ T$. The relative deviation from the integrals (1.2) and (1.4) during that time did not exceed several hundredths of a percent, and the integrals (1.3) remained constant with even higher accuracy.

4. STOCHASTIC PROPERTIES OF THE SYSTEM

The first striking result of the numerical experiments is the randomness of the behavior of the phase

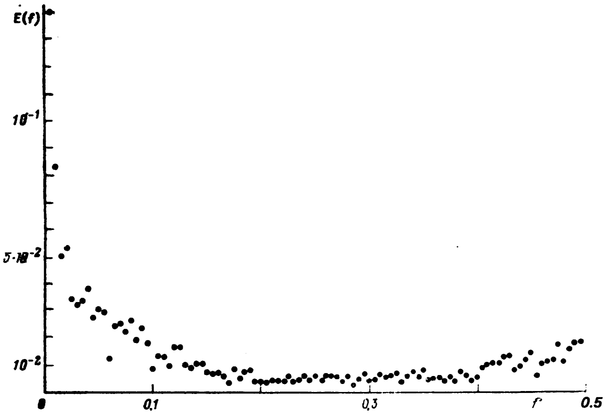

FIG. 4. Energy spectrum of a sequence of states of the system.

trajectories and the equivalence of the different cells belonging to one class (nonconvex or convex configurations). In particular, from time to time the vortex configuration turned out to be close to the initial unstable configuration or to any one of the seven configurations obtained from the initial one by permuting the vortices. Constant transition of the system through an unstable situation is a known stochastization mechanism.[10] Since the time-averaged results corresponding to trajectories with different initial perturbations turn out to be complicated, we present below only data pertaining to the case $\varepsilon=\varepsilon_1$.

To verify that there is no periodicity, we carried out a spectral analysis of the sequence $\xi_l = 10^{-1} + i_l\cdot 10^{-2}$ ($l=1,\ldots,N$), where i_l are the numbers of the cells (from 1 to 14) and N is the number of successive states. It is convenient to reckon this sequence in terms of the values of a time function $\xi(t)$, referred to one second. Figure 4 shows the corresponding energy spectrum $E(f)$ calculated with the aid of a fast Fourier transformation for $N=2$.[13] The absence of sharply pronounced wiggles in the center indicates that the trajectory is not quasiperiodic. Some rise as $f=0.5$ Hz is approached can be attributed to the fact that the oscillations executed by the system of four vortices on going between different configurations are not long-lasting. More accurately, if an oscillation is taken to mean at least one return to the initial state after two steps, then the number of steps participating in the oscillations amounted to 83% of the total number of steps. In this case the average duration of the oscillations turned out to be 2.7 steps, and the average duration of the step $\sim 0.9T$.

We note that one cannot expect cells belonging to two different classes (of convex and nonconvex configurations) to be equivalent. In fact, as shown in Sec. 3, the system executes successive transitions between the two classes, so that it belongs to each of the classes in half of the cases. At the same time, the class of nonconvex configurations breaks up into eight types (cells), and that of the convex ones into six. Thus, in a sequence of states, any particular nonconvex configuration has a lower average frequency than a convex one. In addition, the corresponding phase volume can be different and it is natural to expect a

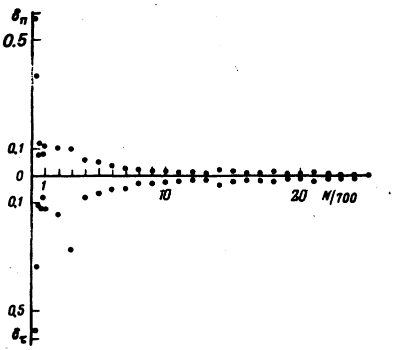

FIG. 5. Settling of the probability distribution into a stationary regime.

difference between the average times of stay of the trajectory in cells of different classes.

The indices $s=6$ and 8 will be used to distinguish between the classes of the convex and nonconvex configurations. Let N_s and T_s be the total number of appearances of configurations of a given class and the corresponding total time. It follows from the foregoing that $2N_6=2N_8=N$, where N is the total number of realized states. Experiment has shown that in 63% of the time the system stays in states with convex configuration $(T_6/(T_6+T_8)=0.63$. Thus, the average time of stay in the system in a state with definite convex configuration is approximately 2.3 times larger than for a nonconvex configuration.

We consider now, for each class, the distributions $w_{i,s}(N)=n_{i,s}N_s^{-1}$ and $q_{i,s}(N)=\tau_{i,s}T_s^{-1}$, where $n_{i,s}$ is the number of the appearances of i-th configuration and $\tau_{i,s}$ is the time of stay of the trajectory in the corresponding cell. To trace the variations of these distributions with increasing N, we introduce the quantity

$$\delta_{n,s}=\sum_i |w_{i,s}(N)-w_{i,s}(N-\Delta N)|$$

and the analogous quantity $\delta_{\tau,s}$ (with w replaced by q). The change from stage to stage was $\Delta N=700$, and it was assumed $\Delta N=100$ within the limits of the first stage. Figure 5 shows the quantities

$$\delta_n={}^1/_2(\delta_{n,6}+\delta_{n,8}),\quad \delta_\tau={}^1/_2(\delta_{\tau,6}+\delta_{\tau,8}).$$

The rapid decrease of these characteristics and the close approach to zero indicate that distributions tend to become stationary. Towards the end of the experiment, the distributions are close to uniform within each class. For nonconvex configuration the probability deviation from uniform distributions of τ and n was only 0.03. For convex configurations, characterized by longer times, the equalization of the distributions was somewhat slower and the deviations from uniformity were 0.8 for τ and 0.06 for n.

To verify the mixing condition, we introduce the probability

$$p_{j,s'}^{i,s}(2m+{}^1/_2|s-s'|)$$

of the transition from the i-th configuration of class s to the j-th configuration of class s' after the number of steps indicated in the parentheses; $m=0, 1, 2, \ldots$; the term $\frac{1}{2}|s-s'|$ reflects the fact that the transitions between different classes are possible only after an odd number of steps, and within a single class only after an even number. The mixing condition means that at large m the following expression should be small (compared with unity)

$$\frac{1}{s}\sum_i\sum_j\left|p_{j,s'}^{i,s}\left(2m+\frac{|s-s'|}{2}\right)-w_{j,s'}\right|=\sigma_{s'}^{s}\left(2m+\frac{|s-s'|}{2}\right). \quad (4.1)$$

The probabilities p and w in (4.1) were calculated from the total aggregate of the N states realized in the experiment. Figure 6 shows the function $\sigma(k)$, defined in terms of (4.1) by means of the formulas

$$\sigma(2m)={}^1/_2[\sigma_6^6(2m)+\sigma_8^8(2m)],$$
$$\sigma(2m+1)={}^1/_2[\sigma_8^6(2m+1)+\sigma_6^8(2m+1)].$$

We see that $\sigma(k)$ decreases quite sharply at first, and at $k>25$ the mixing condition is satisfied accurate to several hundredths. With further increase of k, $\sigma(k)$ decreases slowly and executes small oscillations.

Analogous calculations have shown that if the number of steps is large the probability of the transition satisfies approximately the condition for a Markov process.

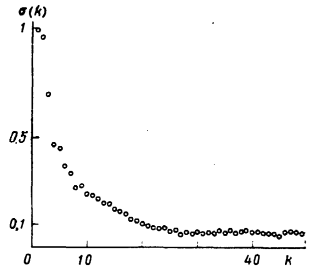

FIG. 6. Mixing in phase space.

5. CONCLUSION

The foregoing analysis of the global stochastic properties of a system of four vortices in conjunction with the established local exponential instability allow us to draw a number of general conclusions.

First, two-dimensional flow of an ideal liquid is in the general case not a fully integrable system (otherwise, quasiperiodicity would have been observed). It is thus impossible in principle to use here the L, A pair method and the technique of the inverse problem of scattering theory, which are successfully to investigate fully integrable systems (see, for example, Appendix 13 of Ref. 6). This conclusion holds also for plasma flow which is two-dimensionalized in a strong magnetic field.

Second, it is natural to expect stochastic properties for a wide class of two-dimensional flows (for example, if the number of discrete vortices is increased and also a continuous vortex field is introduced). This agrees with the random character of the motion of the visualized vortices in liquid helium,[11] and also with the results of numerical experiments with a large number of vortices.[12,13] As to three-dimensional flows, it appears that in the general case the additional effect of the stretching of the vortex filaments will only enhance the stochasticity. As applied to meteorology, one can assume that an important factor, which makes it difficult in principle to forecast the weather, is the stochastic character of the interaction of the cyclones.

One more remark. It is easy to verify that the relative motion of vortices is a Liouville motion, so that it is possible to write down a microcanonical distribution with respect to two invariants of the motion (1.2) and (1.5). The decisive parameter of this distribution in the case of identical vortices is the quantity θ introduced in Ref. 4 (the analog of the temperature). It is of interest to investigate in detail in the future the stochastic properties of the system of four and more vortices so as to verify, for example, the applicability of the microcanonical distribution in a definite range of values of θ (the calculations performed in the present paper correspond to the case $\theta \sim 2.4$).

We are grateful to V. I. Arnol'd and Ya. G. Sinaĭ for a useful discussion of the results and to V. E. Zakharov for a stimulating discussion during one of the stages of the work.

1)A graph is called planar if it can be drawn on a plane (or on a sphere) without self-intersections.

[1]D. Ruelle and F. Takens, Commun. Math. Phys. 20, 167 (1971).
[2]V. E. Zakharov and L. D. Fadeev, Funktsional'nyĭ analiz (Functional Analysis) 5, No. 4, 18 (1971).
[3]E. N. Lorenz, J. Atmos. Sci. 20, 130 (1963).
[4]E. A. Novikov, Zh. Eksp. Teor. Fiz. 68, 1868 (1975) [Sov. Phys. JETP 41, 937 (1975)].
[5]H. Lamb, Hydrodynamics, Dover, 1932. G. K. Batchelor, Introduction to Fluid Dynamics, Cambridge U. Press, 1967.
[6]V. I. Arnol'd, Matematicheskie metody klassicheskoĭ mekhaniki (Mathematical Methods of Classical Mechanics), Nauka, 1974.
[7]G. K. Morikawa and E. V. Swenson, Phys. Fluids 14, 1058 (1971).
[8]G. M. Zaslavskiĭ and B. V. Chirikov, Usp. Fiz. Nauk 105, 3 (1971) [Sov. Phys. Usp. 14, 1 (1971)].
[9]V. M. Alekseev, Matematicheskiĭ Sbornik 76 (118), No. 1, 72 (1968).
[10]Ya. G. Sinaĭ, Funktsional'nyĭ analiz i prilozheniya 2, No. 1, 64 (1968).
[11]G. A. Williams and R. E. Packard, Phys. Rev. Lett. 33, 280 (1974).
[12]B. B. Kadomtsev and D. P. Kostomarov, Phys. Fluids 15, 1 (1972).
[13]Yu. B. Sedov, Izv. Akad. Nauk SSSR Ser. Mekh. Zhidl. i Gaza, 6, 43 (1976).

Translated by J. G. Adashko

Recombination decay of cryogenic helium plasma

V. N. Samovarov and I. Ya. Fugol'

Physicotechnical Institute of Low Temperatures, Academy of Sciences of the Ukrainian SSR, Kharkov
(Submitted 1 March 1978)
Zh. Eksp. Teor. Fiz. 75, 877–892 (September 1978)

An experimental and theoretical study is reported of the kinetics of electron density ($n = 10^{10}$–5×10^{8} cm^{-3}) in helium plasma cooled to cryogenic temperatures ($T_a \lesssim 100$°K). A realistic afterglow model is developed, taking into account electron-temperature relaxation and changes in the density of metastable states. Experiment confirms the existence of the quasistationary decay of electron density, which persists in a broad range of initial dicharge conditions, including the magnetic field. Comparison of experiment with theory has led to the elucidation of the role of hot electrons in cryogenic plasma, to a determination of improved values for the constants of the elementary processes, and, in particular, to a verification of the fact that the temperature dependence of the recombination coefficient of He_3^+ ions is of the form T_e^{-1}.

PACS numbers: 52.25.Lp, 52.80.Hc

INTRODUCTION

When the temperature of heavy particles in helium plasma is reduced from $T_a \approx 300$°K down to cryogenic values, the absolute values of plasma parameters can be investigated in a new range, and new quantitative relationships can be established between them. For example, in decaying plasma, the electron temperature T_e falls to 20–100°K, the density of metastable states may reach $M \approx 10^{13}$ cm^{-3}, and the ratio of M-particle and electron densities rises to $M/n \gtrsim 10^2$ (n is the electron density). There is also a qualitative change in the ion composition of cryogenic plasma. The bulk of the ions consists of the polyatomic ions He_n^+, where $n \geq 3$. The recombination coefficient for these ions is $\alpha > 10^{-6}$ cm$^3\cdot$sec^{-1} and exceeds the recombination coefficients of He^+ and He_2^+, which make up the plasma at room temperature, by a large factor. All this is responsible for many of the features that arise both during the decay of cryogenic plasma and in the cryogenic dc discharge.[1,2]

In the final analysis, the values of the leading plasma parameters and the relationships between them must be traceable to elementary processes (and are ultimately responsible for many aspects of collective phenomena). Sufficient material has now emerged from studies of elementary processes in cryogenic helium plasma to enable us to consider the description of plasma decay as a process of simultaneous variation in its

 0038-5646/78/090444-09$02.40